PHOTOGRAPHIC OBSERVATIONS OF THE CLOUD IN THE NEIGHBOURHOOD OF LIBRATION POINT L_5 OF THE EARTH–MOON SYSTEM

MACIEJ WINIARSKI

Astronomical Observatory of the Jagiellonian University, Krakow, Poland

(Received 22 September, 1989)

Abstract. The paper contains results of three-colour photographic observations of positions and brightness of the cloud in the vicinity of the Earth–Moon libration point L_5. The real character of the images obtained is confirmed by an agreement of their positions on different plates exposed at the same time. The colours of the cloud obtained are essentially different from those of the counterglow. The clouds appeared to be much redder than the counterglow, which may indicate that the particles constituting them are of different nature than those causing the counterglow.

1. Introduction

The presence of clouds in the neighbourhood of libration points L_4 and L_5 of the Earth–Moon system was first reported by Kordylewski (1961). His results were supported by new evidence by Roach (1975) who used a 15-month-long series of measurements from the satellite OSO 6. Roach succeeded also in determining sizes of the clouds, their brightness, and a sequence of positions with respect to the libration points. All the observations of Roach were made in one colour ($\lambda =$ 5000 Å), while the observed objects were in phases 0°, +5° and −5°, i.e. against the counterglow. This paper shows that the libration clouds can be observed photographically, from the surface of the Earth. To carry out such observations during different phases as well as in different photometric systems would contribute to a better understanding of nature of the matter constituting the libration clouds.

2. Detection Conditions for Libration Clouds

Libration clouds are extended objects of low surface brightness. The condition for detection of such an object is that the magnitude difference between a point with combined emission from the object and the background, and a point where emission is due solely to the background, should be greater than some limiting value. This value belongs to the characteristics of the receiver used. If I is the surface brightness of the object, and I_b is the surface brightness of the background, in the linear units (stilbs or S_{10} units), the object will be detected if

$$S = 2.5 \log[(I + I_b)/I_b] > S_{\text{lim}} ,$$

where S_{lim} is a characteristic property of the receiver. Tables I and II give values of S for an object with extra-atmospheric brightness x (in S_{10} units) and of the

Earth, Moon, and Planets **47**, 193–215, 1989.

TABLE I

Observable surface brightness m_x (in stellar magnitude per square degree) and difference object – background (in stellar magnitude) for the object with extra-atmospheric brightness x (in S_{10} units), for different values of the background (in magnitude per square degree), for average observing conditions: altitude 30°, extinction coefficient $0^m.4$

		Background						
x	m_x	1	2	2.5	3	3.5	4	4.5
5	9.05					0.01	0.01	0.02
10	8.30			0.01	0.01	0.01	0.02	0.03
15	7.86			0.01	0.01	0.01	0.03	0.05
20	7.55		0.01	0.01	0.02	0.03	0.04	0.06
30	7.11		0.01	0.02	0.02	0.04	0.06	0.09
40	6.79	0.01	0.01	0.02	0.03	0.05	0.08	0.12
50	6.55	0.01	0.02	0.03	0.04	0.06	0.10	0.15
60	6.35	0.01	0.02	0.03	0.05	0.08	0.12	0.18
100	5.80	0.01	0.03	0.05	0.08	0.12	0.19	0.29
150	5.36	0.02	0.05	0.08	0.12	0.18	0.27	0.41
200	5.05	0.03	0.06	0.10	0.15	0.23	0.35	0.51

corresponding observed brightness m_x (in magnitude per square degree) for various values of the sky background. Table I is calculated for average conditions: the object's altitude 30°, extinction coefficient $0^m.4$; while Table II refers to very good conditions: altitude 50°, extinction coefficient $0^m.2$. It has been assumed here that extinction affects the emission from the object only, rather than that from the background.

The extra-atmospheric brightness x of liberation objects was given by Roach (1975). His measurements were made when the cloud was in opposition (in its full phase). Since the cloud's size exceeds much the size of the Moon, during every

TABLE II

As in Table I, for very good observing conditions: altitude 50°, extinction coefficient $0^m.2$

		Background						
x	m_x	1	2	2.5	3	3.5	4	4.5
5	8.56				0.01	0.01	0.02	0.03
10	7.81		0.01	0.01	0.01	0.02	0.03	0.05
15	7.37		0.01	0.01	0.02	0.03	0.05	0.07
20	7.06		0.01	0.02	0.03	0.04	0.06	0.10
30	6.62	0.01	0.02	0.02	0.04	0.06	0.09	0.14
40	6.30	0.01	0.02	0.03	0.05	0.08	0.12	0.19
50	6.06	0.01	0.03	0.04	0.06	0.10	0.15	0.23
60	5.86	0.01	0.03	0.05	0.08	0.12	0.18	0.27
100	5.31	0.02	0.05	0.08	0.12	0.19	0.28	0.42
150	4.86	0.03	0.08	0.12	0.18	0.27	0.41	0.59
200	4.56	0.04	0.10	0.15	0.23	0.35	0.51	0.72

opposition the cloud is eclipsed with a resulting drop in its brightness. Roach used to eliminate this effect in a calculational way, but introduced some minor errors. Fortunately, these could be readily corrected by referring to the numerical values assumed in the reduction procedure, which Roach scrupulously included in his paper. The diameters of the Earth's umbra and penumbra at the Moon's orbit assumed by Roach were 0°.7 and 1°.2 respectively, while in fact they are two times greater. After taking into account these correct values, the factor used by Roach to correct the objects' brightness for the eclipse effect increased from 1.2 to 1.8; then the brightness value free from the eclipse effects incresed from 20 to 30 S_{10} units, and this is the value to be used in Tables I and II in evaluating whether a particular receiver is capable of detecting a libration cloud. However, one should note that the value x may be different from that of Roach due to dependence of the object's brightness on its phase, physical brightness variation, or employing a photometric system other than that used by Roach.

It is normally assumed that using a photographic plate one cannot get a photometric accurcy better than $0^m.1$. This estimate has been based on the experience with determining star magnitudes from stellar images on plates; but, with steller images, blackening covers just a tiny portion of a plate even in the case of out-of-focus images or images enlarged with the use of 'Schraffier–Kassette', so the accuracy is strongly controlled by local plate inhomogeneities. With the libration clouds, objects of size of several degrees, the case is different: because the blackened areas under comparison are larger, local plate inhomogeneities will be averaged out.

3. Laboratory Test

For the above reasons the observations were preceded by a number of laboratory tests. By choosing different types of plates and ways of developing, it was attempted to get the contrast in the low density region as high as possible. Obtaining a measurable effect for a test object similar to libration clouds does not guarantee a success during actual observations, when there are also noises from background inhomogeneities and atmospheric phenomena. Nevertheless the testing was necessary, as there might have been the case that the investigated object would not produce any distinguishable image even in the laboratory conditions.

Images of photoelectrically calibrated sources of light were measured, averaging densities over circles of 3 mm in diameter, which was the size of a cloud's image on the plate. The plates were exposed for 1 hr, employing sources of light such that the images' densities be 3 to 10 times higher than the veil, which were the conditions quite like those to occur during the actual observations.

Thus there were established the best conditions to be kept to in processing the actual observations:

(1) using Kodak IIaO, IIaF, and ORWO WP1 plates;

(2) developing the plates in the high-contrast, Polish-made developer Fenal;

(3) filtering the developer and using it 24 to 48 hr after preparation;

(4) keeping the developer's temperature at $20° \pm 1°$;

(5) employing the developing times of 6 min for IIaF plates, and 3 min for the other plate types, within accuracy of 15 sec.

Under these conditions, the density difference between images corresponding to objects with magnitude difference as little as $0^m.02 - 0^m.04$ was measurable.

4. Observations

The observations were carried out at the observing station Roztoki Górne in the Bieszczady Mountains ($\lambda = -1^h29^m$, $\varphi = +49°10'$). As averaged over 10 yr, the sky background brightness recorded at the site are: 3.81, 2.94, and 2.05 mag/square degree in the B, V, and red (a system close to R) colour, respectively. The values of the mean extinction coefficient are: for B colour, $0^m.35$; for V colour, $0^m.20$; (for R colour it has not been determined). Comparison of these values with Tables I and II show that, under the circumstances, libration objects could produce a measurable effect.

The observing device consisted of 10 objective lenses from amateur cameras, of focal length from 53 to 85 mm and aperture ratio from 1:1.5 to 1:2. The lenses had been specifically adapted to be used with glass plates of $6.5 * 9$ cm. The so obtained cameras were fixed on a refractor's mounting (200/3000 mm), which served as a guider, ensuring guidance accuracy much better than required. Although the nearest light source was 1 km away, and below the observing stand's level at that, each lens was equipped with a blind, 10 cm deep, similar to sun screens of industrial making, but with an opening angle determined individually to protect it from any diffused light. Observations were made without filters. On IIaO plates one could thus obtain results in the photographic system, but the results of IIaF and WP1 plates corresponded to some indefinite, broad band systems with maxima in yellow and red colour, respectively. But this, obviously incorrect, observational procedure had to be applied due to extremely low brightness of the objects to be observed. Even without any filter, exposition times were about one hour, while the total period during which observations are at all possible is about two hours, due to the proximity of the Moon (no observations can be made when the Moon is above the horizon).

After obtaining in this way a photograph of the region surrounding a libration point, the same region of the sky was photographed with the same camera using the same type of plates during a night when the libration points were not there. The photographs thus obtained (reference plates) were then employed to eliminate any intrinsic sky background enhancement, not related to the position of the Moon, as well as for testing at what level the plate noises are capable of producing apparent, false clouds.

5. Plate Calibration

The exposed plates were calibrated employing a tube photometer. The illumination ratios between consecutive steps of the photometer were determined not from calibrator's apertures but photoelectrically, which ensured a better accuracy. There were two departures from the normal calibration procedure:

(1) The plates were not calibrated immediately after the exposure but only when the weather conditions worsened (sometimes after a few observing nights). Nevertheless, with all the plates the interval between the exposition and the calibration was several times shorter than that between the calibration and the development of the plate.

(2) Exposure times for calibration were considerably shorter than in the actual exposures. Examination of the curve density vs. logarithm of exposure time indicated that the same inclination of the characteristic curve can be obtained if a plate is exposed for 2.5 min (plates IIaO) instead of 60 min, or even for as little as one minute (the other types of plate). Consequently, such short times were used in calibration. This was possible only because the range of considered illumination values was small, by an order of the sky background differences.

Along with exposing the plates, the sky background near the centre of each photographed field was measured. This was necessary to obtain the cloud's brightness from the magnitude difference (per unit area) calculated from the plate. To this purpose, a double astrograph with Ernemann–Ernostar objectives (focal length 285 mm, aperture ratio 1:2) was employed. The objectives worked as photoelectric photometers with Soviet-made photomultipliers FEU 64 for B and V colours and FEU 79 for R colour. The Fabry lenses and diaphragms (constant diaphragms with the field of view's diameter 0°.51) had been installed directly at the photomultipliers, rather than in the usual way. Measurements were made with the instrument fixed in one position by recording a star of known B, V, and R passing across the field of view and next recording the sky background level against the dark current.

If m_b, m_s, l_s, l_b, l_d denote, respectively, the sky background brightness in magn/square degree, brightness (in magnitude units) of the star passing across the field, and the recorded values for the star, the background, and the dark current, then

$$m_b = m_s + 2.5 \log\left(\frac{l_s - l_b}{l_b - l_d}\right) - 1.73 .$$

The constant -1.73 has been introduced to reduce the measurements from the actual diaphragm's area to the area of one square degree.

In this paper the results obtained from 18 plates with libration point L_5 and 36 references plates are presented. The data concerning the libration point plates are collected in Table III, whose consecutive columns give: number of plate within the entire plate collection, middle of the exposure time in UT, exposure duration, geocentric coordinates of the libration point L_5, its altitude above the horizon,

TABLE III

Data about plates with point L_5. The consecutive columns give: number of plate, universal time of observations, exposure duration in minutes, coordinates of point L_5, its altitude, photometric system, obtained background brightness (in magnitude per square degree), phase of the object if it was exactly at point L_5

Number of plate	U.T. $1976^{y}02^{mth}$	exp. [min]	1950.0 α	1950.0 δ	H	Sys.	Background	Φ
277	$18^{d}.756$	60	$8^{h}50^{m}$	12°.6	34°	*r*	1.99	17°
284	$18^{d}.756$	60	$8^{h}50^{m}$	12°.6	34°	*v*	2.84	17°
280	$18^{d}.756$	60	$8^{h}50^{m}$	12°.6	34°	*b*	3.76	17°
288	18.810	46	$8^{h}53^{m}$	12°.4	45°	*r*	1.99	17°
295	$18^{d}.810$	46	$8^{h}53^{m}$	12°.4	45°	*v*	2.84	17°
291	$18^{d}.810$	46	$8^{h}53^{m}$	12°.4	45°	*b*	3.76	17°
298	$19^{d}.808$	66	$9^{h}49^{m}$	8°.0	34°	*r*	1.83	3°
305	$19^{d}.808$	66	$p^{h}49^{m}$	8°.0	34°	*v*	2.98	3°
301	$19^{d}.806$	57	$9^{h}49^{m}$	8°.0	34°	*b*	3.92	3°
309	$19^{d}.860$	55	$9^{h}52^{m}$	7°.7	43°	*r*	1.83	3°
316	$19^{d}.860$	55	$9^{h}52^{m}$	7°.7	43°	*v*	2.98	3°
312	$19^{d}.860$	55	$9^{h}52^{m}$	7°.7	43°	*b*	3.92	3°
329	$20^{d}.860$	63	$10^{h}42^{m}$	3°.0	32°	*r*	1.81	11°
336	$20^{d}.860$	63	$10^{h}42^{m}$	3°.0	32°	*v*	2.93	11°
332	$20^{d}.860$	63	$10^{h}42^{m}$	3°.0	32°	*b*	3.45	11°
340	$20^{d}.914$	51	$10^{h}45^{m}$	2°.7	40°	*r*	1.81	12°
347	$20^{d}.914$	51	$10^{h}45^{m}$	2°.7	40°	*v*	2.93	12°
343	$20^{d}.914$	51	$10^{h}45^{m}$	2°.7	40°	*b*	3.45	12°

photometric system, background intensity in magn/square degree, phase of the libration point. The abbreviations for the photometric system are: b = plate IIaO, background in B system; v = plate IIaF, background in V system; r = plate WP1, background in a system similar to R. The cameras used had the aperture ratio 1:2, and the focal lengths respectively: in systems r and b – 58 mm, in system v – 84 mm. For the plates from the nights of 18/19 and 19/20 February, 1976, the counterglow was present within the field.

6. Plate Measurements

Both the libration points plates and reference plates were measured with a GII photometer of Carl Zeiss Jena making. There was used a square diaphragm of side corresponding to 0.5 mm on the plate; which on the sky gives 0°.5 for b and r system and 0°.34 for v system. In making photometric profiles, the step between consecutive measurements was such that the measured fields did not overlap. Some part of information was thus lost, but individual measurements could be independent from each other. Constancy of the step was assured by means of a wheel with 400 slits, mounted on the screw driving the plate. The slits were counted photoelectrically, and after some fixed number of slits a measurement was released.

If during any measurement a stellar image or plate defect entered the diaphragm's field, the measurement was qualified as invalid. The decision on the validity were up to the observer. The fact that this process of decision making could not be automatized is certainly a major drawback of the method. The limiting stellar magnitude below which a measurement was eliminated depended not only on the particular plate but also on the point measured (the further away from the center of the field, the brighter stars were indistinguishable). As a rule, the limiting value was 7^m to 9^m, while Roach eliminated stars up to $V = 5^m.5$. The results of measurements, after converting the current signals into voltage ones, were registered at a Polish-made PSPD-90 microcomputer.

Photometric profiles were carried out along circles of equal declination. Before and after every profile the veil was measured. The density as against the veil is calculated as

$$D = \log \frac{I_w}{I},$$

where I_w is the reading of the microphotometer at the veil, and I is the reading at the profile. There are two ways possible: to measure the veil at the profile's extension, off the exposed part of the plate, or to measure the veil at some fixed point of the plate. The veil value may depend, in a systematic way, on position on the plate. By measuring the veil at the profile's extension this dependence is eliminated, while by measuring at some fixed point it is transferred as a systematic error to the density map. Therefore the former procedure is a more correct one, however, it entails larger random errors whereas any *random* error of the veil for a given profile becomes a *systematic* error for the entire profile. So there is a possibility that entire profiles on the density map will be translated by some constant value with respect to the other ones.

So there was adopted the following procedure. Before and after each profile the veil was measured at the extensions of the profile, I_{w1}, and at a fixed point of the plate, I_{w2}. Let us define, for each profile i, a function $f(i)$ such that

$$f(i) = \frac{I_{w1}(i)}{I_{w2}(i)}.$$

By fitting a second-order polynomial to the shape of $f(i)$ for each plate using the least-square method, the function $\overline{f}(i)$ was then obtained. Eventually, for the profile i the veil value $I_w(i)$ was taken as

$$I_w(i) = I_{w2}(i) * \overline{f}(i).$$

Thus any systematic dependence of veil on the profile's number was taken into account, and the systematic errors for individual profiles were reduced to the errors in determining the veil at some fixed point.

With the veil so assumed, a surface brightness map for each plate was calculated from

$$X(i, k) = g[I_w(i)/I(i, k)] .$$

The quantity g is the function of (I_w/I) determined for each plate from the tube photometer marks as a second-order polynomial. Surface brightness values $X(i, k)$ constituted a brightness map of size 56 per 64, where the index i ran along declination, and index k – along right ascension. The map $X(i, k)$ is determined up to a constant value, since with a tube photometer it is not possible to establish the zero point of the scale.

7. Reduction of Systematic Errors

The map of quantities $X(i, k)$ was freed from the errors of dependence of illumination on the distance from the plate's centre (field error). The error was determined by calculating

$$W(r) = \bar{X}(\emptyset) - \bar{X}(r) ,$$

where r is the distance from the plate's centre to the point measured, and $\bar{X}(r)$ is the mean value of $X(i, k)$ for the regions with distance to the centre within r and $r + 1$. Since $W(r)$ is a characteristic feature of individual cameras, $\bar{W}(r)$ was calculated as an average of $W(r)$ over all photographs made with one camera. It was assumed here that any other effects (sky background variation, counterglow, libration objects) would average out. The functions $\bar{W}(r)$ are shown in Figure 1. The field error is a strong effect. If the manner of removing it had not been quite

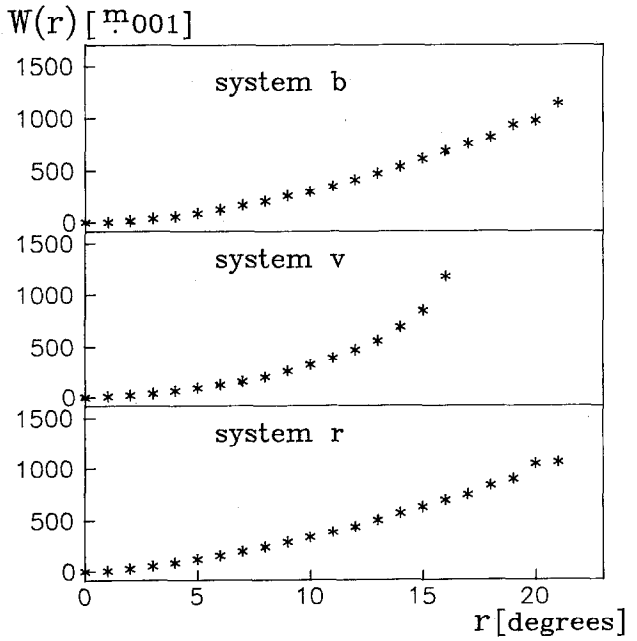

Fig. 1. Field error for the cameras used in the systems b, v, r.

adequate, there could have resulted a false object; yet such an object would have been symmetrical with respect to the plate's centre.

For each plate the map of quantities $Y(i, k)$, corrected for the field error, was calculated from

$$Y(i, k) = X(i, k) + \bar{W}(r) .$$

The next reduction step consisted in eliminating any large-scale variation of illumination (e.g. in the direction from or towards the horizon). It was done by fitting the best possible plane to the quantities $Y(i, k)$: $i * A + k * b + C$ using the least-square method. After establishing parameters A, B, C for each plate, the fitted plane was subtracted from the measurements $Y(i, k)$, which gave the map $Z(i, k)$:

$$Z(i, k) = Y(i, k) - i * A - k * B - C .$$

The effectiveness of the reduction from $X(i, k)$ to $Y(i, k)$ and from $Y(ik, k)$ to $Z(i, k)$ is shown in Table IV, whose columns 3, 4, 5 give, for three exemplary plates, values of dispersion (in units of 0.001 mag) as calculated from the data of the tables X, Y, Z.

The maps of quantities $Z(i, k)$ do not take into account any information on the cloud's size and possibility of averaging the data over regions comparable to this size. Such an averaging was made and regions of enhanced brightness situated along the ecliptic were found. The regions were considerably larger than the objects observed by Roach and occurred both on the plates with libration points and on the reference plates. These were not objects related to the libration points but bright features connecting the zodiacal light with the counterglow. Their presence obscured any possible effect from libration clouds.

In order to remove these large-scale effects, the following procedure was adopted. Maps $Z(i, k)$ were diminished by discarding measurements at points more than 18° away from the plate's centre (which corresponded approximately to the position of the libration point). It was reasonable, because at that distance the number of measurements on which the reduction of the map $X(i, k)$ to $Y(i, k)$ was based, considerably fell off, with the resulting increase in the reduction error. The

TABLE IV

Dispersions of the surface brightness maps (in units 0^m001) for three exemplary plates, illustrating the effectiveness of the reduction procedures

Number of plate	Sys.	Dispersion of the map			
		X	Y	Z	A
277	r	238	129	85	20
284	v	332	83	54	13
280	b	239	102	54	10

cloud should be found on the diminished map too, as none of 32 positions given by Roach was more than 11° away from the libration point.

Next, for each point of the map $Z(i, k)$ there were calculated differences between the mean value of $Z(i_1, k_1)$ for all points (i_1, k_1) whose distance to (i, k) was smaller than a fixed value R_1 and the mean value of $Z(i_2, k_2)$ for all points (i_2, k_2) whose distance to (i, k) was greater than R_1 and smaller than R_2. The value R_2 was matched to R_1 in such a way that the area of a circle of radius R_1 be equal to the area of a ring with radii R_1, R_2. The idea of this procedure is given in Figure 2. There are shown, in a projection onto a plane passing through an imaginary object, what the results of the procedure for objects of different sizes are. If the radius of the object is R_1 (libration cloud), then its brightness will not change after the procedure, while the brightness of an object of greater size will become less. If an object is so large that its brightness variation within limits $2 * R_2$ can be approximated with a straight line, then after the procedure it will disappear altogether. In practice, as the value R_1 is known only from the paper of Roach, and not too exactly at that ($R_1 = 3°$, while Roach's instrument counted photons over a field of diameter 2°, which determined the resolving power), circles of various R_1 and corresponding R_2 were fitted to every individual point (i, k). Radius R_1 took values 1.5, 1.9, 2.4, and 2.9 degrees. For each (i, k), the largest obtained difference for different R_1 values was taken as an element of the matrix $A(i, k)$, which was the outcome of the procedure.

In other words, as a model of a cloud, there was assumed a cylinder of radius R_1, and, by varying R_1 within some limits, it was attempted to get a cylinder as

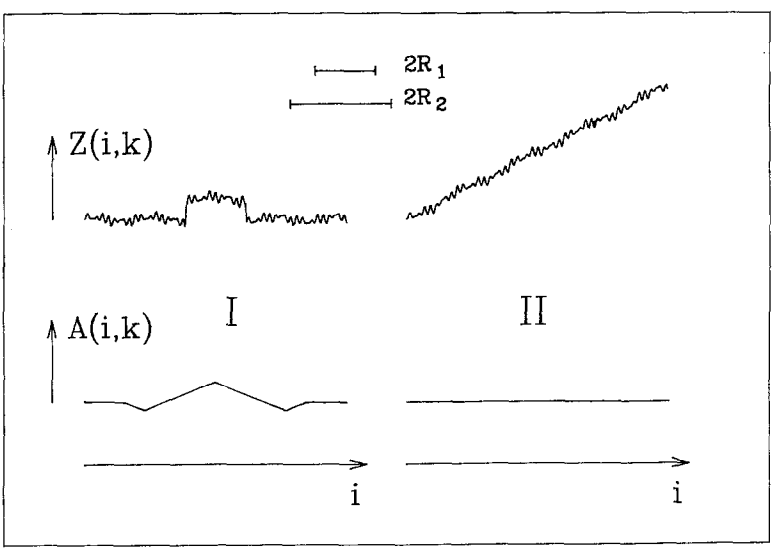

Fig. 2. The effect of replacing the maps $Z(i, k)$ with the maps $A(i, k)$: (I) for an object of size of a libration cloud, (II) for an object of considerably greater size.

high as possible in respect to its neighbourhood. Performance of this procedure for each point (i, k) in turn as a centre of the cylinder's base, gave a map of best cylinder's lengths $A(i, k)$. The obtained mean dispersions for maps $A(i, k)$, $0^m.012$, $0^m.017$ and $0^m.015$ for b, v, and r system respectively, are an evidence of efficiency of the procedure, which both averages data over the area of circle R_1 and removes any effects of greater dimensions. Dispersion for $A(i, k)$ should be regarded as a purely formal parameter, since the elements of $A(i, k)$ are not independent from each other.

8. Possibility of 'False Objects'

The maxima found at the maps $A(i, k)$ may be:

(1) artifacts due to the plate noise,
(2) intrinsic, constant brightness enhancements within the sky background,
(3) effects produced in the Earth's atmosphere,
(4) the actual objects sought.

In order to evaluate the probability that the effects observed could be due to the plate noise the following procedure was adopted: The maps $A(i, k)$ were divided into disjoint domains of size $i = k = 12$, which corresponded to the maximum value of $2 * R_1$ used previously in fitting the cylinder. Thus values $A(i, k)$ in one subdomain are independent of values $A(i, k)$ in other subdomains. Since the overall size of the maps $A(i, k)$ was $56 * 64$, the number of elements within some subdomains (situated near the boundaries) was less than $12 * 12$, depending on the starting point of the division. Moreover, the elements $A(i, k)$ are not specified for the map's points further than 18° from the optical centre. It was decided that subdomains containing less than N_1 elements $A(i, k)$ would not be considered at all. By the way of definition it was assumed that there was an object within a given subdomain if at least N_2 elements contained in it satisfied the condition

$$A(i, k) > \bar{A} + N_3 * \sigma ,$$

where $\bar{A}$ and σ denote the mean value and dispersion of the total map $A(i, k)$. The values N_1, N_2, and N_3 are chosen arbitrarily by the observer, thus the definition is of an essentially subjective character; yet its assumption allowed to estimate the probability that the object so defined could be just an artifact produced incidentally by the plate noise. The establishing that the objects are of actual nature consisted in finding their coincidences within the same domains on different plates exposed at the same time.

Let there be MM plates representing the same region of the sky. Let us introduce a division (common for all the maps $A(i, k)$) into subdomains (i.e., specify the initial values i, k for the division). Next, assume some values for N_1, N_2, and N_3. Then for each plate j, $j = 1, \ldots, MM$, there is defined $C\emptyset(j)$ – total number of the subdomains without those containing less than N_1 elements, and $C(j)$ – number of subdomains within which there is an object following the definition assumed.

The probability of incidental generating of an object within some chosen subdomain on the plate j is

$$P(j) = C(j)/C\emptyset(j) .$$

The probability of incidental generating of an object within some chosen subdomain on at least least m plates is

$$P'(m) = \sum_{j=m}^{MM} (-1)^{(j-m)} \binom{j-1}{m-1} S_j ,$$

where S_j is the sum of probabilities of coincidence of j events $P(i_1), \ldots, P(i_j)$ over all possible combinations of events $i_1, \ldots, i_j$ such that $i_1 < i_2, \ldots < i_j$. As the events consisting in that there is an object within some given subdomain on two different plates are independent of each other, the probability of coincidence of the events is equal to the product of individual probabilities of these events. Hence,

$$P'(m) = \sum_{j=m}^{MM} (-1)^{(j-m)} \binom{j-1}{m-1} \sum_{*} \prod_{l=1}^{j} P(i_l) ; \tag{1}$$

where $\sum_{*}$ denotes summing over all $\binom{MM}{j}$ combinations $i_1 \ldots i_j$ such that $i_1 < i_2 < i_j$.

Definite values for N_1, N_2, N_3 were assumed as well as a specific division into subdomains. For each of the observation nights, 18/19, 19/20, and 20/21 February, there is 6 plates exposed simultaneously. The fact that the plates were made in different photometric systems is ignored here. The plates exposed during the same night can be well regarded as simultaneous ones, since the variation due to the orbital motion between successive exposures is less than two columns of the map $Z(i, k)$, while in constructing the map $A(i, k)$ the values are averaged over 6 to 12 columns. For each six plates from one night, one determines a subdomain within which the object sought, as defined before, appears on the possibly greatest number of plates m_1. According to formula (1), the probability $P'(m_1)$ is calculated, that in the given collection of 6 plates, an object may be generated incidentally on m_1 plates.

The value $P'(m_1)$ depends on a particular division into subdomains (i.e. on the point from which the division was started). In order to remove this effect, the maps $A(i, k)$ were divided in number of different ways and then the mean value of $P'(m_1)$ was taken. The values $P'(m_1)$ obtained for each of the three observing nights are given in Table V.

The values $P'(m_1)$ are dependent on the assumed values of N_1, N_2, N_3. Probability $P'(m_1)$ is calculated for a subdomain selected beforehand rather than the one within which the object appears on most plates. To meet these objections, analogous calculations (for the same N_1, N_2, N_3) were performed for the reference

TABLE V

Probability P' of an incidental generation of the object observed and L – ratio specifying how many times it is more probable that the object observed on the reference plates could have arisen incidentally as compared with that observed on the libration point plates

Date	$N1 = 48$; $N2 = 3$; $N3 = 2.5$		$N1 = 48$; $N2 = 1$; $N3 = 3$	
$1976^{y}02^{mth}$	$P'(m_1)$	L	$P'(m_1)$	L
18/19	0.01146	1.3	0.03382	0.8
18/19*	0.00863	2.4	0.03026	3.2
19/20	0.00086	23.0	0.00079	23.5
20/21	0.00146	4.8	0.00145	3.9

plates of each night. Let us denote as mm_1 and $P'(mm_1)$ quantities corresponding to m_1 and $P'(m_1)$, obtained for the reference plates. Quantities $L = PP'(mm_1)/P'(m_1)$, given in Table V, specify how many times it is more probable that the object observed on the reference plates could have arisen incidentally as compared with that observed on the libration point plates.

For the nights of 19/20 and 20/21 February, for two assumed definitions of a cloud (i.e. triples of N_1, N_2, N_3) the object on the plates with libration points appears as much more real than the object on the reference plates. Moreover, for different divisions of map $A(i, k)$ into subdomains, the object on the libration point plates appeared at the same place (to an accuracy of one subdomain), while on the reference plates, the location of the object depended strongly on the division.

For the plates from the night of 18/19 February, the results are different. Possiblilities of incidental generaton of apparent objects on the liberation point plates and on the reference plates are practically the same. The objects on the libration point plates appear at the same place (location A) for different divisions into subdomains, but the location of the object-like effect on the reference plates also does not depend on the division (location B). The locations A and B are evidently different. If one removes the subdomains containing location A from the libration point plates, then the object to be found on most of the plates appears at the location B. As the location B: $\alpha = 8^{h}15^{m}$, $\delta = +0\overset{\circ}{.}7$, is situated in the region of the plates that is nearest to the Milky Way, it was suggested that there is some intrinsic, constant brightness enhancement which appears both on the libration point plates and on the plates of reference. Therefore, all the calculations were repeated after discarding the region surrounding the location B both from the libration point plates and from the reference plates. The values obtained, which in Table V are indicated as 18/19*, show that also for the plates of 18/19 February an incidental generating of an object-like effect at the location A is not likely, and the object can be regarded as an actual one.

The results given in Table V refer to all the plates, without any selection, including a plate (No. 288) with a distinct manufacturing defect. The values $A(i, k)$

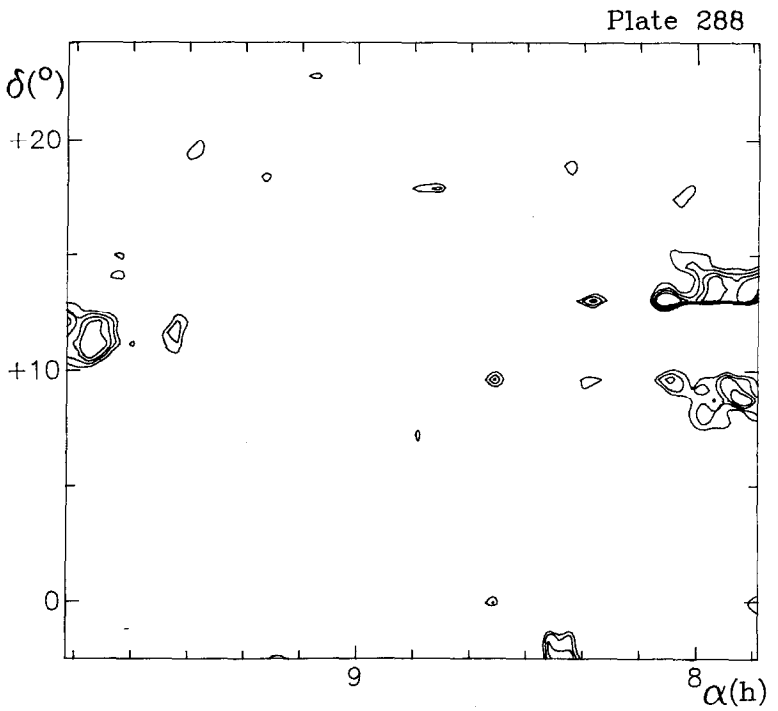

Fig. 3. The map of quantities $A(i, k)$ for a plate with a distinct emulsion defect. The lowest isophote corresponds to the value $A(i, k)$ exceeding the mean value of $A(i, k)$ by 2σ. Subsequent isophotes are drawn by every $\frac{1}{2}\sigma$.

for that plate are presented in Figure 3, where the lowest isophote corresponds to the level by $2 * \sigma$ above the average, and the next ones are drawn every $\frac{1}{2}\sigma$. It can be seen that there appear three bright false objects (not confirmed on any other plate) with sharp boundaries parallel to the equator (and so to one of the plate's sides), which is an indication that the features are due to inhomogeneities in the plate's sensitivity. The inclusion of that plate resulted in diminishing the values of L in Table V for the night of 18/19 February. It is manifest that even the presence of a plate evidently defected in the procedure did not prevent providing an evidence for the existing object.

The objects appearing on the plates from the nights of 18/19 (in position A), 19/20 and 20/21 February are not due to the plate noise. Nor are they intrinsic constant features at the sky, since then they would have been registered on the reference plates as well as it was the case with the object in position B from the night of 18/19 February. It is also unlikely that they could have orginated within the Earth's atmosphere, as their presence has been confirmed by subsequent exposures. The time interval between the exposures ($1\frac{1}{2}$ hr) can be well neglected when considering the libration point's motion, while it is hardly probable for an object-like effect produced in atmosphere to remain steady in its position against the stars during all that time, augmented still by the plate's exposure time.

From *a priori* considerations, the observed enhancements could be objects related rather to the ecliptic and not to the Moon's orbit. Although a replacment of the maps $Z(i, k)$ with the maps $A(i, k)$ removes any large-scale effects, it is still possible that there could be some brightness enhancements of sizes within the considered range in the vicinity of the ecliptic. Such objects have been actually found (Maucherat *et al.*, 1986); yet they are situated very close to the anti-solar point (within 3°) and are not always observable. In fact, objects of this kind are visible on some of the reference plates which include the anti-solar point in their field: for instance, on plate 404 (r system), the map $A(i, k)$ of which is shown in Figure 4. However, if the enhancements observed near the point L_5 were related to the ecliptic instead, then they would be equally likely to appear on the libration point plates as on the reference plates, which as it can be seen from Table V, is not the case.

Figure 5 shows, by the way of example, the maps $A(i, k)$ for the plates from the night of 19/20 February. Although at some of the maps there are enhancements brighter than the enhancement at the position $\alpha = 8^h53^m$, $\delta = +17°3$ the fact that the latter appears on all the plates is an indication that it is a real one.

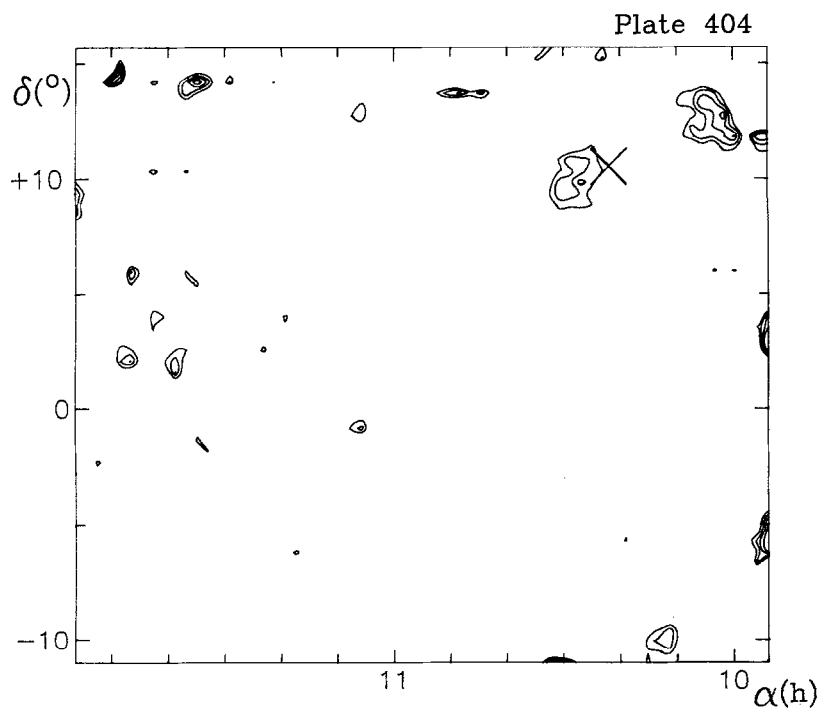

Fig. 4. The map of quantities $A(i, k)$ for a reference plate including the counterglow in its field. There are visible brightness enhancements of small size near the centre of counterglow, which is marked by ×.

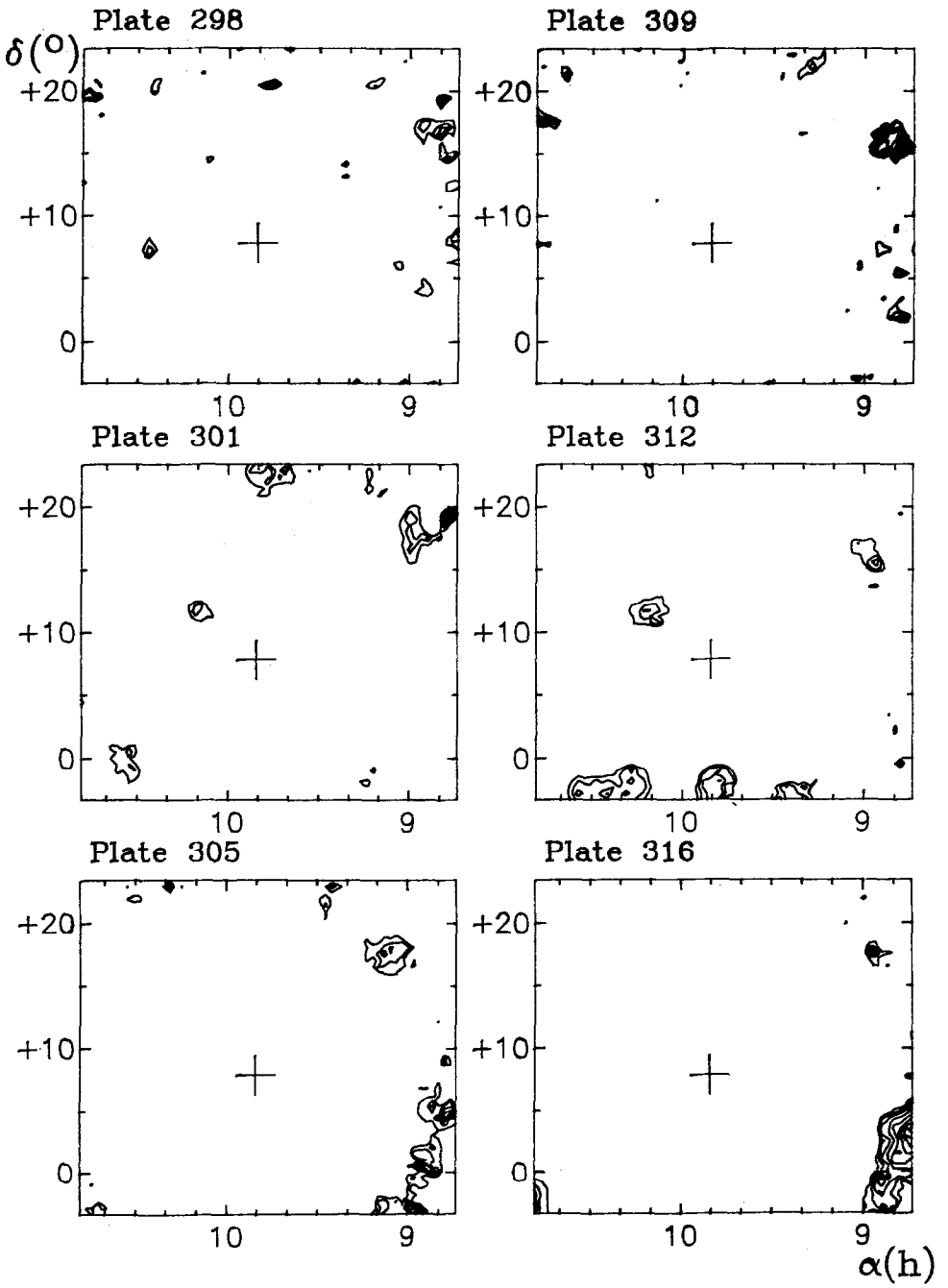

Fig. 5. The maps for the plates from the night of 19/20 February. Isophotes as in Figure 3. + denotes the position of point L_5. The brightness enhancement in the upper right-hand corner of the maps, appearing on all the plates, is the libration object.

9. Results

For each of the nights, 18/19, 19/20, and 20/21 February, there were brightness enhancements on the maps $A(i, k)$, which could not be accounted for otherwise than by assuming that they were due to objects accompanying the libration points. The positions of each object was determined as the arithmetic mean of indices $\bar{i}$ and $\bar{k}$ for those (i, k) for which $A(i, k)$ exceeded the mean value of $A(i, k)$ by more than 3σ. The results remained practically the same when the criterion was altered to 2σ, 2.5σ, and 3.5σ, respectively (only for night of 19/20 the position in right ascension varied depending on the criterion adopted, but the variation was of less than 10 min). The equatorial coordinates of the observed object, averaged over all plates from each night (except for plate No. 288), are given in Table VI, which contains also the coordinate differences between the object and libration point L_5. If one calculates the mean error in position, it is small (0°.5 to 1°.4), but one must have in mind that it is determined from too small a number of plates; moreover the values $A(i, k)$ are not independent from each other, so the error is underestimated. Taking this into account, it can be assumed that the object's positions in respect to the point L_5 for the nights of 18/19 and 19/20 are the same, whereas for the night of 20/21, the object in right ascension is by 20 min closer to the point L_5. The object is situated very close to the central region of counterglow and the bright star α Leo. For this discrepancy the following explanations are plausible:

(1) During the night of 20/21 one observed a local brightness enhancement within the counterglow, as in Figure 4. An argument against such an interpretation is that the object observed is distinctly brighter than the brightness enhancement within the central region of counterglow.

(2) During the night of 20/21 one observed the diffused light from α Leo. As α Leo did not produce any distinguishable object-like effects on the reference plates, the observed enhancements must have been due to diffusion on the matter of libration clouds. It may be a peripheral part of the cloud, which while not illuminated by any bright star is not visible at all, and thus not included into the objects of nights of 18/19 and 19/20.

TABLE VI

Positions of the cloud near point L_5

Date 1976	Observed object		Object – L_5	
	α 1950	δ	$\Delta\alpha$	$\Delta\delta$
$18^{d}/19$	$8^{h}02^{m}$	+20°.6	-50^{m}	+8°.1
19/20	$8^{h}53^{m}$	+17°.3	-57^{m}	+9°.5
20/21	$10^{h}10^{m}$	+11°.7	-34^{m}	+8°.9
Counterglow				
20/21	$10^{h}13^{m}$	+11°.0		
α Leo	$10^{h}06^{m}$	+12°.2		

It is most likely that the observed brightness enhancement is due to a superposition of a libration cloud and an enhancement produced by both the mechanisms suggested above.

The positions obtained for libration object are more distant from L_5 than those of Roach, but the rule found by him that during winter months the object is further off the Moon than the libration point is still valid.

The brightness of the clouds observed was determined in the following way. For each of the maps $A(i, k)$, the maximum value of $A(i, k)$ within a circle of radius 2°.9 and centre coinciding with the cloud's positions as given in Table VI was determined. The radius corresponded to the maximum radius of the circle over which the values $Z(i, k)$ had been averaged in calculating $A(i, k)$, which diminished the accuracy of determining the object's position. The maximal value of $A(i, k)$ thus obtained was then taken as Δm, magnitude difference between a point with the emission both from the cloud and the background and a point where emission is due solely to the background. The mean value of Δm was adopted for both plates exposed in one system during one night (only for r system the plate No. 288 of night of 18/19 was discarded). With the background brightness determined from photoelectric measurements (Table III) and the corresponding brightness X_b in S_{10} units, the observed brightness of the cloud X, in S_{10} units, was calculated from

$$X = X_b * (10^{0.4*\Delta m} - 1) .$$

In order to obtain the extra-atmospheric brightness of the cloud, X_0, the value X was corrected for atmospheric extinction effect, with the mean extinction coefficients determined from a few scores of nights: 0m.35 in b-system and 0m.20 in v-system. For r-system the value 0m.1 was adopted, which resulted from extrapolating the extinction coefficients from the other systems. Values of Δm, X, X_0 are given in Table VII.

There is a possibility that Table VII contains systematic errors, which could have arisen in the following way. Sky background values determined from photoelectric

TABLE VII

Values of the cloud's brightness near point L_5 for photometric systems r, v, b. Δm denotes the cloud's brightness against the background (in magnitude), X, X_0 – observed and extra-atmospheric brightness of the cloud (in S_{10} units), $\Delta m'$ – brightness of the central region of the counterglow with respect to the surrounding ring

Date 1976y02mth	Δm			$X[S_{10}]$			$X_0[S_{10}]$		
	r	v	b	r	v	b	r	v	b
18/19	0.053	0.067	0.034	80	46	10	90	58	15
19/20	0.044	0.101	0.026	77	63	7	86	79	10
20/21	0.030	0.070	0.036	53	45	14	60	58	22
		$\Delta' m$							
Centre of counterglow	0.020	0.017	0.017						

measurements are practically in V, B, R systems, whereas photometric systems involved in getting Δm values are defined by the spectral sensitivity curves of the plates used. They are shown in Figure 6, together with the sensitivity curves for the systems V, B, R. As it can be seen, only for blue colour, the photographic and photoelectric systems are in conformity with each other. In the other colours there are distinct disparities between the systems.

The value X and X_0 in Table VII are correct only provided that Δm as obtained from the plate is equal to the (unknown) value $\Delta m'$ in the photoelectric system corresponding to this plate. This is the case only when the energy distributions in spectra of the objects under comparison (libration object and background) are the same. If we assume this, values X_0 in Table VII are correct. Similarly as for the counterglow, the dependence of the libration object's luminosity on wavelength can be expressed as

$$\frac{X_0}{k * I_\odot} = \lambda^\beta \quad \text{or} \quad \log \frac{X_0}{I_\odot} = \beta \log \lambda + \log k ,$$

where $I_\odot$ the solar radiation intensity in wave-length λ in any units, k – factor converting these units to S_{10} units. Values 4400 Å, 5500 Å, and 6400 Å were taken as effective wave-lengths for systems b, v, and r, respectively; $I_\odot$ was taken from Johnson (1960), and X_0 – mean values from Table VII for each system.

The dependence of $X_0/I_\odot$ on λ is presented in Figure 7, where the point corresponding to $\lambda = 5000$ Å and $X_0 = 30S_{10}$, the mean value obtained by Roach, has been marked. Roach's observations were made during a maximum of solar

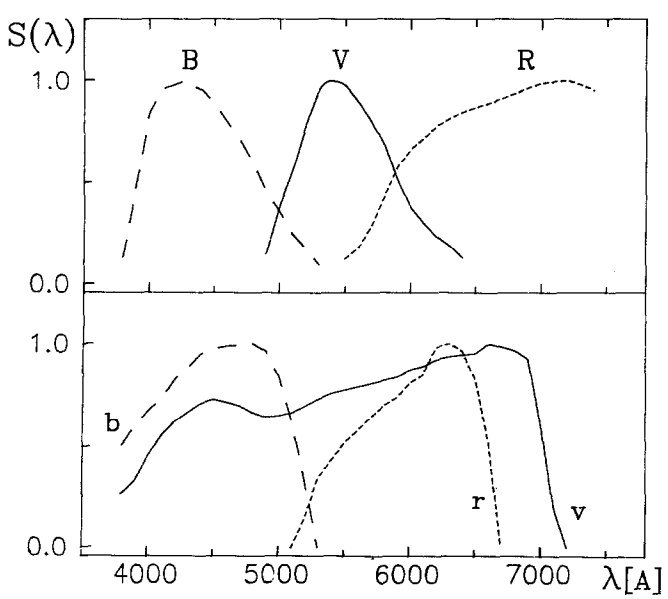

Fig. 6. The spectral sensitivity curves for the photographic plates used (systems b, v, r) as compared with photoelectric systems B, V, R.

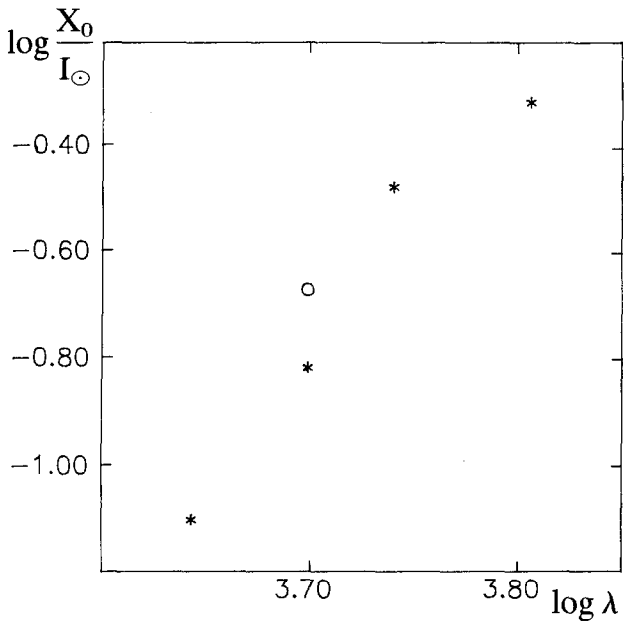

Fig. 7. Dependence of $X_0/I_\odot$ on wave-length. The light circle denotes the result of Roach after assuming that the cloud's brightness on solar activity.

activity, while the observations from this work – during a solar minimum (the respective mean spot numbers are 103.6 and 4.3 (Coffey and McKinnon, 1988)). If the libration object brightness depends on the level of solar activity, as it is the case with the counterglow (Robley, 1979), then in 1976 the brightness should be by 40% greater than in the time of Roach's observations, thus for $\lambda = 5000$ Å one should have the value $42S_{10}$ (light circle in Figure 7). For the values $30S_{10}$ and $42S_{10}$, respectively, one has the coefficient $\beta = 4.8$ and $\beta = 5.6$, values distinctly different from those obtained for the counterglow $-2 < \beta < -1$ (Gingilis, 1962). Hence, it can be concluded that the spectral distribution for the light coming from the libration cloud is different from that of the counterglow.

This result can be supported in a qualitative way basing directly on the Δm values from Table VII, without using the photoelectric background values. This excludes the possibility that the result originates from the discrepancy between the photographic and photoelectric systems. It was proceeded as follows: for the plates with visible counterglow the position of its brightest region was determined, with the assumption that this position cannot be more than 5° off the anti-solar point (Tanabe, 1965). The brightness of the central part of counterglow against the sky background could not be determined (Δm in Table VII) because the plate area was too small for the counterglow and the counterglow-free background to be included on the same plate. Therefore we chose to measure $\Delta' m$ – the difference between the central part of counterglow (of 15° in diameter) and the surrounding part forming a ring of the same area. If the spectral distributions of the counterglow

and of the libration cloud were the same and equal to $f(\lambda)$, then the brightness (in units of S_{10}) for the libration cloud X_L, central part of counterglow X_{gc} and counterglow ring X_{gr} could be given as

$$X_L = a * f(\lambda); \quad X_{gc} = b * f(\lambda); \quad X_{gr} = c * f(\lambda) ,$$

where the constants a, b, c are independent of wavelength.

Let us have sky background S with a spectral distribution $S(\lambda)$ (in units of S_{10}). Then for the libration cloud against the background

$$\Delta m = 2.5 \log \frac{X_L + S}{S} = 2.5 \log\left(1 + \frac{X_L}{S}\right) =$$

$$= 2.5 \log\left(1 + a \frac{f(\lambda)}{S(\lambda)}\right). \tag{2}$$

For the central part of counterglow against the surrounding ring

$$\Delta' m = 2.5 \log \frac{X_{gc} + S}{X_{gr} + S} = 2.5 \log\left(1 + \frac{X_{gc} - X_{gr}}{X_{gr} + S}\right) =$$

$$= 2.5 \log\left(1 + (b - c) * \frac{f(\lambda)}{c * f(\lambda) + S(\lambda)}\right).$$

In the spectral ranges v and r the background is considerably brighter than the counterglow, so it can be assumed that $c * f(\lambda) + S(\lambda) = S(\lambda)$ and

$$\Delta' m = 2.5 \log\left(1 + \frac{(b - c) * f(\lambda)}{S(\lambda)}\right). \tag{3}$$

From the formulae (2) and (3), taking after Table VII the mean values of Δm as 0.079 for v and 0.042 for r, and the values $\Delta' m$, one obtains $a * f(\lambda)/S(\lambda)$ and $(b - c) * f(\lambda)/S(\lambda)$. The ratio of these quantities, $a/(b - c)$, should not depend on λ, whereas it is equal to 4.8 for v-system, and 2.1 for r-system. Thus the assumption that the spectral distributions of light from the libration cloud and that from the counterglow are the same has led to a contradiction with the observational evidence.

10. Discussion and Conclusions

The relation obtained between brightness and wave-length for the libration objects is distinctly different from that of the counterglow. Since the observations of libration objects were made in phases close to 0° (as were obviously those for the counterglow) the difference can be due solely to a different nature of the diffusing particles in either case (chemical composition, size, shape). This is what could be expected. If we discard the old, visual estimates of the counterglow's parallax

(Astapovich, 1958), these should be located at distances of the order of several astronomical units from the Earth. The dust at these distances is a product of distintegration of comets (Fechtig, 1987), while the dust present in the vicinity of libration points is most probably the matter scattered in the effect of meteorites hitting the Moon's surface. So it is clear that these dust particles would be of quite different nature. A priori it is also possible that, in the vicinity of libration points there are some gas concentrations; and thus the spectral distribution different from that of the counterglow could be accounted for by the presence of gas emission lines. Yet any gas component would have been very rapidly forced out of the cloud by radiation pressure and solar wind, and there is no obvious mechanism available to replace it. For an observational falsification of the gas component hypothesis, a close examination of the cloud's spectrum is needed. There were actually such tests made for the airglow line, 5578 Å, in the counterglow (Tanabe, 1965). To perform analogous observations for the libration clouds is much more complicated, as the clouds can be even by more 10° off the libration point and the short period when the observations are possible is not sufficient for inspecting all possible positions where the cloud could be. The observational method used in this paper is not suitable for immediate (during one observation night) determination of the cloud's position because processing the plates requires much time. Possible use of a CCD camera instead of plates would allow for a rapid determination of the cloud's position as well as for accurate positioning of a spectrograph or any other small-field observing device.

Application of CCD cameras would permit also to perform observations that involve reducing light intensity, as photometry with filters or polarization measurements. Such observations cannot be done with plates due to their low sensitivity. However, a disadvantage of using CCD detectors is their small field as compared to the area of the sky to be surveyed in searching for the libration clouds.

The method employed in the present work, i.e. using a number of parallel cameras with plates as receivers of light should enable one to proceed with the following programs:

(a) For observations covering a sufficiently large phase interval one can get (for different photometric systems) a brightness-phase relation and compare it either with the results of Mie's theory (van der Hulst, 1951) or with the experimental data (e.g. Giese, 1979). This will allow one to specify what kind of particles the cloud cannot be made of. For instance, the very fact that the cloud's brightness increases with wave-length for phases close to 0° (Figure 7) stands in contradiction to the relation calculated for scattering on uniform spheres with refractive index 1.55 and radii less than the wave-length (van der Hulst, 1951);

(b) When comparing observations corresponding to the same phase but made at very different times one can find if there is any long-term variation of the cloud's brightness and if it is correlated with such a variation in the brightness of the counterglow (Robley, 1979) or, possibly, with solar activity. So we compared our observations made in 1976 with the observations by Roach from 1969–70.

Within that period the counterglow brightness increased by 40%. Unfortunately, both the value given by Roach and that augmented by 40% (by assumption that the cloud's brightness changed in the same way as the brightness of counterglow) agree equally well with the value interpolated from our obesrvations (Figure 7). Comparison of values obtained from observations made at very different times but in the same system is still needed for settling the issue of long-term brightness variation.

Acknowledgments

My thanks are due to local inhabitants in the Bieszczady mountains, forest officers and workers, as well as Frontier Guard soldiers for their assistance in the construction and maintenance of the Bieszczady observing station. Without their help the present work would not have been possible.

I am also grateful to Dr M. Jerzykiewicz for his critical remarks to the manuscript, in particular for directing my attention to the possibility of distorting the cloud's image by α Leo star during the night of 20/21 February.

The present work was partially financed within the program RPBR I-11-1-05. The calculations in part were made at a computer donated by the Princeton University.

References

Astapovich, I. C.: 1958, *Astron. Tsirk.* **190**, 25.
Coffey, H. E. and McKinnon, J. A. (eds.): 1987, Solar-geophysical Data prompt reports, 516-1.
Fechtig, H.: 1987, *Publ. Astr. Inst. of Czechoslovak Acad. Sci.* **67**, 253.
Giese, R. H.: 1979, *IAU Symposium* No. 90, Solid Particles in the Solar System, 1.
Gindilis, L. M.: 1962, *Astron. Zhurn. Akad. Nauk SSSR* **39**, 93.
Johnson, F. S.: 1960, *Solar Radiation in Satellite Environment Handbook*, Lockheed Missiles and Space Division.
Kordylewski, K.: 1961, *Acta Astr.* **11**, 165.
Maucherat, A., Llebaria, A., and Gonin, J. C.: 1986, *Astron. Astrophys.* **167**, 173.
Roach, J. R.: 1975, *Planet. Space Sci.* **23**, 173.
Robley, R.: 1979, *IAU Symposium* No. 90, Solid Particles in the Solar System, 33.
Tanabe, H.: 1965, *Publ. Astron. Soc. Japan* **17**, 339.
van der Hulst, H. C.: 1957, *Light Scattering by Small Particles*, John Wiley, New York.